Received: 15 March 2021 | Accepted: 17 September 2021

DOI: 10.1111/2041-210X.13752

Methods in Ecology and Evolution BRITISH ECOLOGICAL SOCIETY

RESEARCH ARTICLE

Characterizing individual tree-level snags using airborne lidar-derived forest canopy gaps within closed-canopy conifer forests

Jessica M. Stitt[1] | Andrew T. Hudak[2] | Carlos A. Silva[3] | Lee A. Vierling[4] | Kerri T. Vierling[1]

[1]Department of Fish and Wildlife Sciences, University of Idaho, Moscow, ID, USA

[2]Rocky Mountain Research Station, Forest Service, US Department of Agriculture, Moscow, ID, USA

[3]School of Forest Resources and Conservation, University of Florida, Gainesville, FL, USA

[4]Department of Natural Resources and Society, University of Idaho, Moscow, ID, USA

Correspondence
Jessica M. Stitt
Email: jstitt@uidaho.edu

Funding information
NSF Idaho EPSCoR Program; Idaho Space Grant Consortium; NASA Carbon Monitoring System Program, Grant/Award Number: NNH15AZ06I

Handling Editor: Ryan Chisholm

Abstract

1. Airborne lidar is often used to calculate forest metrics about trees, but it may also provide a wealth of information about the space between trees. Forest canopy gaps are defined by the absence of vegetative structure and serve important roles for wildlife, such as facilitating animal movement. Forest canopy gaps also occur around snags, keystone structures that provide important substrates to wildlife species for breeding, roosting and foraging.
2. We wanted to test a method for quantifying canopy gaps around individual snags and live trees, with the working hypothesis that snags would have more gaps surrounding them overall than live trees. We evaluated canopy gaps around individual snags (n = 270) and live trees (n = 2,186) and evaluated correlations between canopy structure and snag occurrence in dense conifer stands of the Idaho Panhandle National Forest, United States. We paired airborne lidar with ground reference data collected at fixed-radius plots (n = 53) to evaluate local gap structure. The R package ForestGapR was used to quantify canopy gaps throughout the canopy to determine where the differences were greatest. A canopy space profile was created for each tree by mapping gaps (a) vertically every 2 m in height (2–50 m above-ground), and (b) horizontally across small (16 m^2), medium (36 m^2) and large (64 m^2) footprint sizes.
3. Our results suggest that this method is robust for quantifying canopy gaps around individual trees. The canopy space profiles were distinctly different for snags and live trees, with more canopy gaps within the area surrounding snags relative to live trees. The greatest differences occurred at mid-canopy heights (~20 m above-ground) and at the smallest footprint size (16 m^2).
4. These results show potential to improve the understanding of gap dynamics in closed-canopy conifer forests, and we suggest that snag modelling could be improved by incorporating lidar-derived canopy gap analyses alongside existing methodologies.

KEYWORDS

airborne laser scanning, forest canopy gaps, forest gap analysis, gap fraction, individual tree level, lidar, remote sensing, snags

1 | INTRODUCTION

Standing dead trees (hereafter, snags) are keystone structures that play a disproportionately large role in wildlife community composition and dynamics across forest systems (Tews et al., 2004). Structurally, snags provide unique ecological substrates for wildlife in breeding, roosting and foraging (Bunnell et al., 1999; Cockle et al., 2011; Drever et al., 2008; Gentry & Vierling, 2008; Martin & Eadie, 1999; Mikusiński et al., 2001), with species reliant on the standing deadwood or microhabitats contained within (including nest cavities, bark fissures and other structures; Asbeck et al., 2020; Larrieu et al., 2018; Martin et al., 2004). Snags serve as useful indicators of biodiversity (Basile et al., 2020; Michel & Winter, 2009; Paillet et al., 2017), with snag densities and distributions supporting an array of species across many taxonomic groups, including birds, mammals, amphibians, reptiles (Bunnell et al., 1999; Drever et al., 2008; Drever & Martin, 2010; Martin et al., 2004; Titus, 1983), invertebrates (Bunnell et al., 1999; Hanula et al., 2006; Janssen et al., 2011) and fungi (Bunnell et al., 1999; Jackson & Jackson, 2004). Additionally, snags differ from live trees in their roles regarding carbon storage and sequestration (Curtis, 2008; Powers et al., 2013; Russell et al., 2015), nutrient cycling (Lovett et al., 2010), wildfire fuel loading (Powers et al., 2013; Ritchie et al., 2013) and structural heterogeneity of forest stands (Hansen et al., 1991; Martinuzzi et al., 2009). As snags harbour a wealth of information about forest function, accurately characterizing snag sizes and distributions across a landscape is therefore of high interest for studies and management activities that cross multiple disciplines.

Lidar (light detection and ranging) has improved scientists' ability to describe 3D forest characteristics remotely and may enhance the quantification of snag sizes and distributions for many applications. Airborne lidar (also airborne laser scanning or ALS) is a tool well suited for mapping forest structure, as it provides 3D scans of the canopy structure from above, which can be analysed at varying resolutions—from the landscape scale (~10^2–10^5 km^2) to individual trees (e.g. Eitel et al., 2016; Falkowski et al., 2009; Goetz & Dubayah, 2011; Guo et al., 2017; Vierling et al., 2008). Most previous lidar work on remote detection of snags has been carried out at two levels: the survey plot level (~0.04–1 ha) and the individual tree level (~1–10 m^2). At the plot level, progress has been made in predicting probable snag densities and distributions using airborne lidar structural metrics (Bater et al., 2009; Martinuzzi et al., 2009) and intensity data (Wing et al., 2015). At the individual tree level, a focus on segmentation of individual trees (isolating one crown from surrounding crowns) has provided great insights into volume and biomass calculations (Kankare et al., 2013; Klockow et al., 2020; Krzystek et al., 2020; Popescu et al., 2003; Putman et al., 2018; Yao et al., 2012). Both scales of analysis have been applied to wildlife management in the form of habitat mapping for individual species (e.g. Casas et al., 2016; Vogeler & Cohen, 2016).

While focusing on individual tree crown-level metrics is powerful, forest canopy structure consists of not only crowns but also the space between crowns, often referred to as canopy gaps (Shugart, 1984; Urban et al., 1987). Canopy gap characteristics are important features of a forest environment, and recent methodologies have been developed to better quantify gap dynamics through space and time using lidar-based approaches (e.g. Silva et al., 2019). Structurally, snags have a three-dimensional shape that differs from live trees, lacking the green vegetation characteristic of crowns and retaining only the sparser yet coarser woody components of branches and trunks. Within a lidar point cloud, an absence of points need not equal an absence of information, and canopy gap analysis provides a promising avenue for further refinement of snag detection methods and subsequent wildlife habitat mapping based on information about the spaces between trees. For instance, birds fly through and therefore utilize the empty space between tree crowns, so it is more holistic and perhaps accurate to think of both the space occupied by tree crowns and the unoccupied space when characterizing suitable or preferred wildlife habitat.

To evaluate whether airborne lidar data can capture differences in the proportion of empty gap space surrounding snags and live trees (known as gap fraction), we analysed two features of the vertical and horizontal gap space around individual snags and live trees: height above-ground (representing a vertical perspective) and size of gap around a given tree (representing the horizontal space). Our main objective is to quantify how canopy gap profiles differ between snags and live trees, such that canopy gap profiles could potentially be used as an indicator of snag presence. We hypothesize that snags should have distinct canopy gap space profiles due to the loss of foliage and branches, and we would expect snags to have greater total gap area than live trees. We compare the vertical and horizontal gap characteristics around snags and live trees within closed-canopy conifer stands. From a vertical perspective, we would expect these characteristics to differ most in the mid-canopy; in the lower canopy, we would anticipate fewer gaps due to forest structures such as saplings, shrubs and/or stumps. In the higher canopy, we would anticipate fewer gap differences between live trees and snags due to the conical shape of conifer tree crowns, as both decrease in woody and needle biomass approaching the top of the tree. From a horizontal perspective, we would expect that there is an optimal footprint size that captures the gaps that are associated with an individual tree. No other studies to our knowledge have used this approach at the individual-tree level or applied it to snags. Therefore, this method may hold promise for describing canopy gap structure that might correlate with snag presence.

2 | MATERIALS AND METHODS

2.1 | Study area

The study was conducted in closed-canopy forest stands within the Idaho Panhandle National Forest (IPNF), Idaho, United States. The study area consisted of two sites within IPNF: one site in the Coeur d'Alene River Ranger District (herein CdA) and one site in the Saint Joe Ranger District (herein StJ; Figure 1). Both sites are

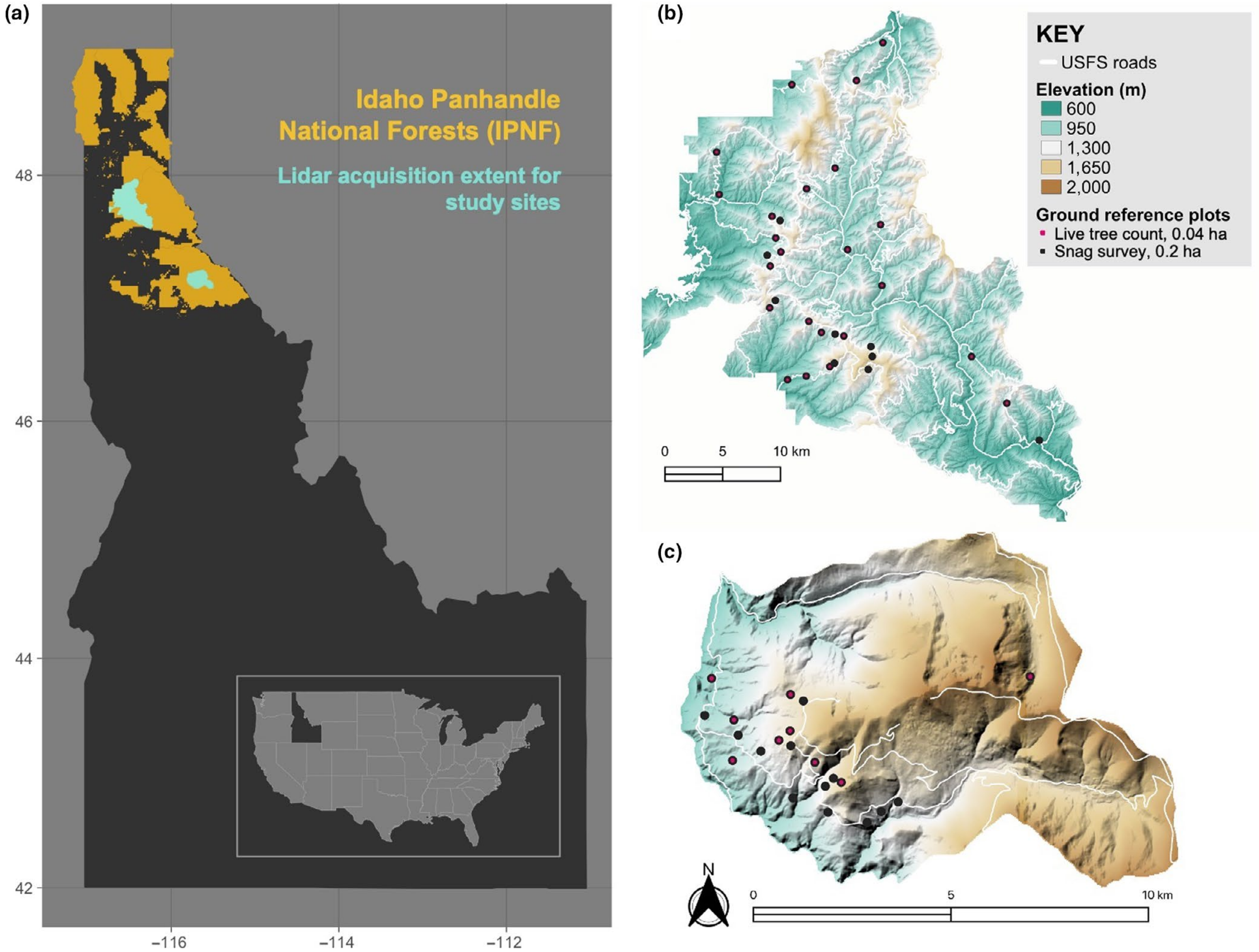

FIGURE 1 Map of the study sites. (a) Study area within Idaho Panhandle National Forests (IPNF) in northern Idaho, United States. There were two lidar acquisitions in the IPNF where all ground reference survey data were collected: within the (b) Coeur d'Alene River (CdA) and (c) Saint Joe (StJ) Ranger Districts. Please note the different scales for each site. Across the two sites, there were a total of 53 25-m radius ground reference plots with snag surveys (0.2 ha; black circles), and 32 of those contained 11.3-m radius subplots (0.04 ha; pink dots) with live tree counts

composed of mature mixed-conifer forest stands managed for multiple uses, including timber production, recreation and wildlife habitat (IDFG, 2016). At CdA, the most abundant live tree species were grand fir *Abies grandis*, western hemlock *Tsuga heterophylla* and Douglas fir *Pseudotsuga menziesii*. At StJ, the most abundant live species were grand fir, western red cedar *Thuja plicata* and western larch *Larix occidentalis*. Across both sites, the most abundant species of snags found were grand fir and western larch, followed by Douglas fir at CdA and western redcedar at StJ.

2.2 | Field measurements

To map snags within closed-canopy forest, ground reference surveys were conducted within 25-m fixed-radius plots at each site. Survey plot locations were selected through a stratified random sampling design based on canopy cover and height metrics from lidar and constrained using criteria to enable subsequent point count surveys of forest birds, based on existing protocols (e.g. Dudley & Saab, 2003; Vogeler et al., 2013) including a 300-m minimum distance from other plot centres and a road buffer (minimum of 60 m and maximum of 250 m away from roads). Plot centres were recorded using a global navigation satellite system (GNSS) receiver (Trimble GeoXH; accuracy <1 m) and differentially corrected in post-processing. We surveyed each plot for snags within a 25-m radius (0.2 ha plots), recording only snags taller than 1.37 m (to measure diameter at breast height, DBH) and with a DBH >15 cm, based on minimum diameter for nesting by regional woodpecker species (Schroeder, 1983). Information on snag condition was recorded including DBH, tree species (when possible), height and spatial coordinates. Coordinates were determined using the same handheld Trimble GNSS receiver as used for plot centres, positioned on the north side of each bole. Coordinates for each snag were then centred by subtracting half the measured DBH from the northing value to correct for placement bias.

2.3 | Lidar data acquisition and preprocessing

Discrete-return ALS data were acquired across both sites as part of an ongoing effort by the U.S. Forest Service Rocky Mountain Research Station (USFS RMRS) to develop advanced protocols for forest mapping and monitoring. Details on the lidar acquisition parameters can be found in Table 1. The georeferenced lidar data were processed at the plot level using the R environment (R Core Team, 2020, version 4.0.3). Point clouds were preprocessed using the LIDR package (Roussel et al., 2020) at a 50-m radius around plot centres (0.8 ha plots) to generate buffered, height-normalized, filtered and pit-free canopy height models [CHMs; following methods similar to Silva et al. (2016)] with 0.5-m spatial resolution, as depicted in Figure 2a. CHMs were then clipped to the 0.2-ha plot level for canopy gap analyses.

2.4 | Individual tree and forest canopy gap detection

The 0.8-ha pit-free, filtered, height-normalized CHMs were also the basis for individual tree detection (ITD) methods used to generate a list of live tree locations to compare against ground reference snag locations per 0.2-ha plot, as live trees were not surveyed at the 0.2-ha scale. However, a subset of plots from each site was sampled by USFS RMRS in 2017 simultaneously, providing a count of live trees within 11.3-m fixed-radius subplots (0.04 ha; also centred on plot centre). As GNSS coordinates were not collected for live trees, these counts of live trees per subplot were used to calibrate ITD methods to improve the accuracy at the 0.2-ha scale. To account for possible error originating from lidar unable to fully penetrate dense forest stands, the count data were filtered by height (or DBH where height was not recorded) to create three versions per subplot: all live trees, only live trees >20 m tall or with DBH ≥20 cm and only live trees >30 m tall or with DBH ≥20 cm. Four iterations of ITD were run using the RLIDAR package (Silva et al., 2019), via segmentation based on local maxima within a fixed window size. The minimum height threshold was held constant (2 m), but fixed window size (surrounding pixel extent used to estimate local maxima) was altered by iteration: 3 × 3, 5 × 5, 7 × 7 and 9 × 9 pixels. ITD was performed across the full 0.8-ha CHM raster associated with survey plots and then clipped to the 0.04-ha subplot extent. Each iteration of ITD estimates was compared against the three versions of filtered counts, and the difference in live tree count per subplot (filtered—ITD) was used to evaluate the relative error of ITD estimations (Table 3A). Average error per subplot by site was used as the

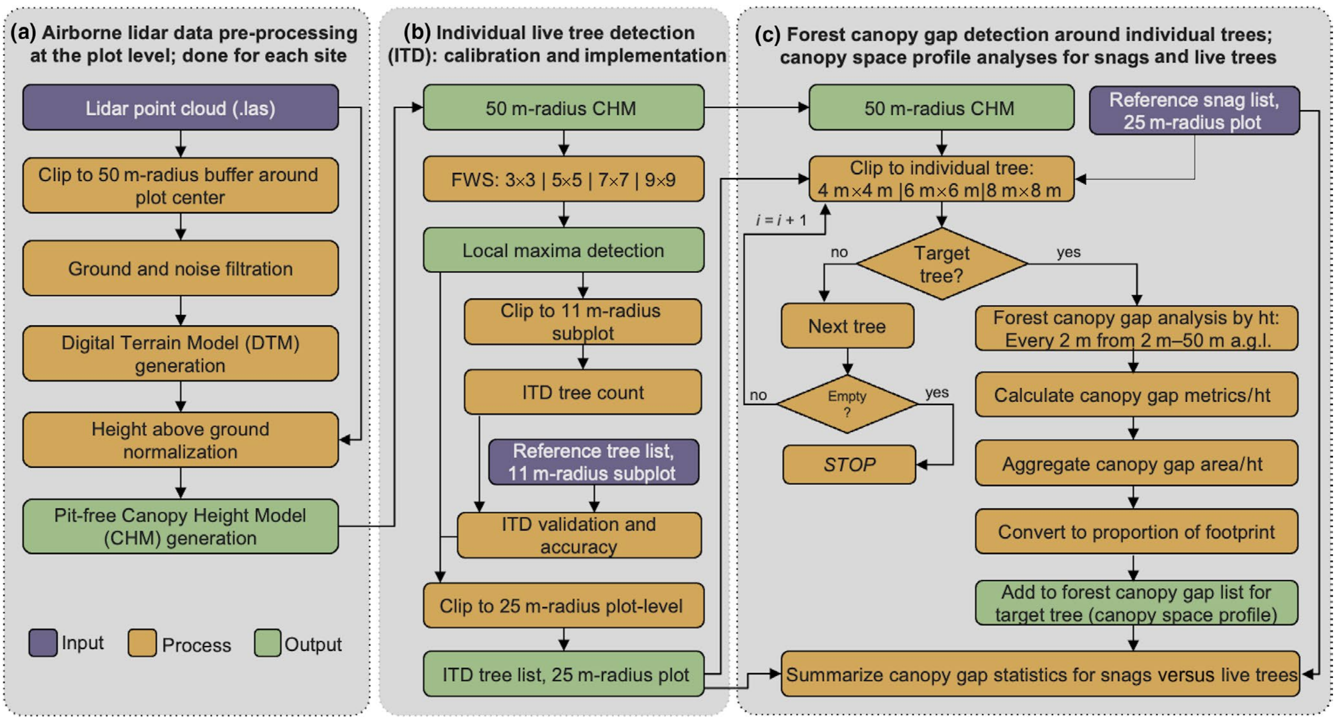

FIGURE 2 Workflow of the airborne lidar data processing for canopy gap profile generation using the FORESTGAPR package. Overview of the inputs, processes and outputs to go from the point cloud to the canopy gap profile around individual trees. (a) Sitewide lidar data were pared down to the ground reference plot level and processed to generate a canopy height model (CHM) for each plot. (b) Live trees sampled within a subset of plots were used to calibrate individual tree detection (ITD) algorithms used to generate a list of live tree locations for each plot to compare against a list of reference snag locations obtained from field surveys. FWS stands for fixed window size, which was the focus of the ITD calibration. (c) Forest canopy gap detection was carried out around individual trees using ForestGapR, and canopy gap profile statistics were generated and summarized across all snags and all live trees to determine whether profiles differed significantly between the two groups

accuracy metric to determine the best configuration to expand to the 0.2-ha scale (Table 3B). Please see Figure 2b for an overview of the ITD process.

TABLE 1 Airborne lidar acquisition parameters. The discrete-return airborne lidar (also airborne laser scanning, ALS) data from the two study sites for this paper (based on two IPNF Ranger Districts: Coeur d'Alene River, CdA; Saint Joe, StJ) were part of a larger acquisition carried out by USFS RMRS in 2016 (see Fekety et al., 2018 for more details). The lidar extent of CdA spanned 78,706 ha to the east of Coeur d'Alene, ID, USA (centred at 47°44′40.0″N, 116°36′38.8″W). The lidar extent of StJ spanned 7,598 ha to the east of Avery, ID, USA (centred at 47°08′28.5″N, 116°05′38.9″W)

Parameter	Specification
Date collected	12 October 2016
Vendor	Atlantic Group, LLC
Sensor	Leica ALS70-HP
Flight altitude	1,965 m above-ground level
Flight speed	110 kts
Pulse frequency	278 kHz
Scan frequency	41 Hz
Scan angle	±30°
Swath width	1,098 m
Swath overlap	50%
Laser wavelength	1,064 nm
Laser beam divergence	0.22 mrad
Vertical accuracy	5.9 cm
Footprint diameter	43 cm
Nominal pulse density	4.2 pulses/m^2

To evaluate canopy space profiles around live trees and snags, the coordinates for the centre of each ITD-generated tree & each reference snag were used in conjunction with the 0.8-ha CHM rasters for each plot and analysed with the ForestGapR package (Silva et al., 2019). The size threshold for canopy gap detection was set to all gaps ≥1 m^2 total area at the given canopy height, and three sizes of square clips were made from CHM rasters around each tree centre: 4 m × 4 m (16 m^2), 6 m × 6 m (36 m^2) and 8 m × 8 m (64 m^2; hereafter referred to as footprint sizes: small, medium and large, respectively). Square clips were used (vs. circular clips) to preserve maximum data from the 0.5-m resolution raster, and the sizes were chosen to encompass the range of average crown diameters for these sites. Canopy gap area per square was calculated from the sum of all gaps for each footprint size. These repeated measures of canopy gap extent at different footprint sizes were used to study how canopy gap area changes across spatial scales.

For each tree, canopy gap area was also calculated over multiple canopy heights, creating a stack of 2D square clips, with a minimum height of 2 m above-ground (to omit noise below breast height) and a maximum height of 50 m above-ground (determined from tallest trees in census), and measured every 2 m to ensure full coverage of the vertical canopy profile. This stacked approach was used to study how canopy gap area changes through vertical space. Pairing the three footprint sizes with the stacked heights enabled the investigation of both vertical and horizontal dimensions of canopy gaps around individual snags and live trees (Figure 3). This approach provided 75 gap area measurements around each tree (across the small, medium and large footprint sizes over 25 heights, from 2 to 50 m above-ground). Please see Figure 2c for an overview of canopy gap profile generation.

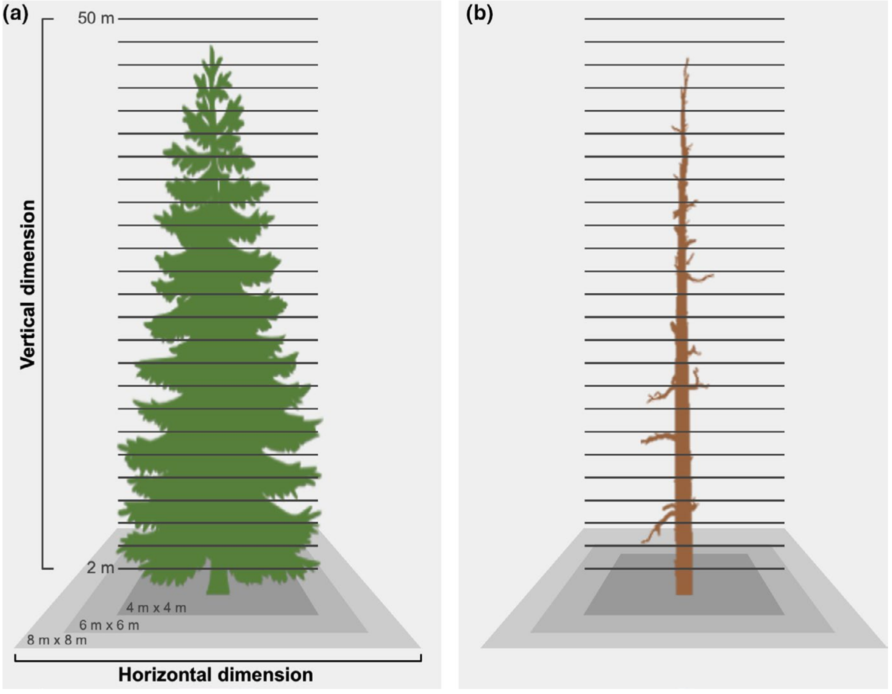

FIGURE 3 Canopy gap profiles. Illustration of the vertical and horizontal dimensions of forest canopy gap detection for (a) live trees and (b) snags. The vertical dimension encompasses gap analyses run every 2 m above-ground from 2 m to 50 m into the forest canopy. The horizontal dimension incorporates three footprint sizes centred on each tree, including a small size (4 m × 4 m), medium size (6 m × 6 m) and large size (8 m × 8 m). Compiling canopy gap fractions across 25 heights over three footprint sizes (75 data points per tree) created a canopy gap profile for each tree that was used to analyse differences in gap dynamics between snags and live trees

2.5 | Individual snag and canopy gap analysis

For each 2D square, the canopy gap area was divided by footprint area to calculate canopy gap fraction to standardize values across footprint sizes. The response variable for statistical tests was canopy gap fraction per 2D square. Mean (±*SE*) gap fractions were calculated for live trees versus snags across three categorical predictor variables: site (CdA or StJ), footprint size (small, medium, large) and canopy height (2 m–50 m above-ground). Differences in mean gap fraction between tree types (snag–live) were also calculated across the same three predictor variables. Footprint size and height above-ground were treated as repeated measures, with unique trees as the unit of observation. Data did not meet assumptions of normality, so nonparametric tests were used to compare canopy gap fractions between groups. We used Mann–Whitney *U* tests to evaluate differences between group means by tree type across all combinations of predictor variables, at a significance level of 5%. All statistical analyses were conducted using the R environment (R Core Team, 2020, version 4.0.3).

TABLE 2 Summary statistics for all plots and trees in the study. All reference snags and ITD-generated live trees included in analyses were within 0.2-ha survey plots, located at one of two sites within the Idaho Panhandle National Forests: Coeur d'Alene River (CdA) or Saint Joe (StJ) Ranger Districts. Averages are shown with standard error in parentheses

Attribute	CdA	StJ
Plots, total	32	21
Elevation (m)	675–1,545	1,041–1,668
Snags, total	180	90
Average snags/plot	6 (±1)	4 (±1)
Range of snags/plot	0–23	0–12
Live trees, total	1,187	999
Average live trees/plot	37 (±2)	48 (±4)
Range of live trees/plot	12–66	22–85

3 | RESULTS

At the 0.2-ha survey scale, there were 270 snags total across 53 ground reference plots, with an average density of five snags per plot (Table 2). A subset of 32 of the 53 ground reference plots contained 0.04-ha subplots with census data, with a total of 538 live trees used to calibrate ITD methods (Table 3). Results of the ITD accuracy assessment found that the 7 × 7 fixed window size was the

TABLE 3 Accuracy of live tree estimation across multiple configurations of tree census data and ITD parameters. To calibrate the individual tree detection (ITD) methods used for this study, we compared individual tree counts from field-derived census data and lidar-derived ITD data across the same spatial extents. Field-derived census data consisted of ground survey counts of all live trees within fixed-radius circular subplots (0.04 ha) across both study sites, but did not include GNSS-based coordinates of each tree. Lidar-derived ITD data were used to estimate live tree central coordinates within subplots, based on canopy height models (CHM; 0.5 m grid cell) built from airborne lidar data as the basis for ITD-generated estimates of tree locations within each subplot (via segmentation using local maxima within fixed window sizes). Aggregated by study site, Table 3A shows (a) the summary statistics for the field-derived census counts (mean number of trees per subplot ±*SE*) across three variations used to filter tree counts based on height threshold; and (b) the summary statistics for the lidar-derived ITD counts (mean number of trees per subplot ±*SE*) repeated across four different fixed window sizes (in pixels) for each subplot. Table 3B shows the error rates in live tree estimation (mean error per subplot ±*SE*) calculated as the differences between field-derived census counts and lidar-derived ITD counts across three height filters and four fixed window sizes (ITD count − census count). Negative numbers represent an underestimation, and positive numbers represent an overestimation of trees per subplot. The configuration with the smallest difference in tree count was used for further analyses; for both sites, this configuration was the same: a 7 × 7 (pixel) fixed window size for ITD paired with census data filtered to include only trees >30 m tall (bolded in table)

(A)	(a) Census count, by height filter			(b) ITD count, by fixed window size			
Study site (# of subplots)	All live trees	Trees >20 m tall	Trees >30 m tall	3 × 3	5 × 5	7 × 7	9 × 9
CdA (23)	16 ± 1.6	9 ± 1.2	7 ± 1.1	18 ± 0.9	10 ± 0.7	8 ± 0.6	6 ± 0.5
StJ (9)	20 ± 2.4	12 ± 2.4	9 ± 2.2	14 ± 1.0	11 ± 0.9	9 ± 0.9	7 ± 1.0

(B)		Error in live tree estimation (ITD—census count)		
Study site	Fixed window size	All live trees	Trees >20 m tall	Trees >30 m tall
CdA	3 × 3	1.8 ± 1.4	8.3 ± 1.2	10.3 ± 1.1
	5 × 5	−5.6 ± 1.2	0.9 ± 0.9	2.9 ± 0.7
	7 × 7	−8.0 ± 1.2	−1.5 ± 0.9	**0.5 ± 0.7**
	9 × 9	−9.4 ± 1.1	−3.0 ± 0.8	−1.0 ± 0.7
StJ	3 × 3	−5.3 ± 1.8	2.4 ± 1.7	4.9 ± 1.7
	5 × 5	−8.4 ± 1.8	−0.7 ± 1.7	1.8 ± 1.6
	7 × 7	−10.7 ± 1.7	−2.9 ± 1.5	**−0.4 ± 1.4**
	9 × 9	−12.2 ± 1.6	−4.4 ± 1.4	−2.0 ± 1.3

most accurate for both sites and performed best when used with census data filtered to only include trees >30 m tall, with a total average overestimation of 0.2 trees per plot (Table 3). The 7 × 7 fixed window size was applied to plots at both sites, and subsequent ITD estimation of live trees at the 0.2-ha survey scale generated a total of 2,186 live tree locations across 53 plots, with an average density of 41 trees per plot (Table 2).

A total of 184,200 square-shaped, vertically distributed slices of canopy were analysed from 2,456 individual trees. Please see Figure 4 for a visualization of canopy gap profiles around a live tree and snag. Snags were surrounded by a greater fraction of canopy gap than live trees (13% greater overall; $p < 0.001$). At the predictor variable level, live trees and snags differed in the canopy gap fractions surrounding them across heights, sites and footprint sizes, with

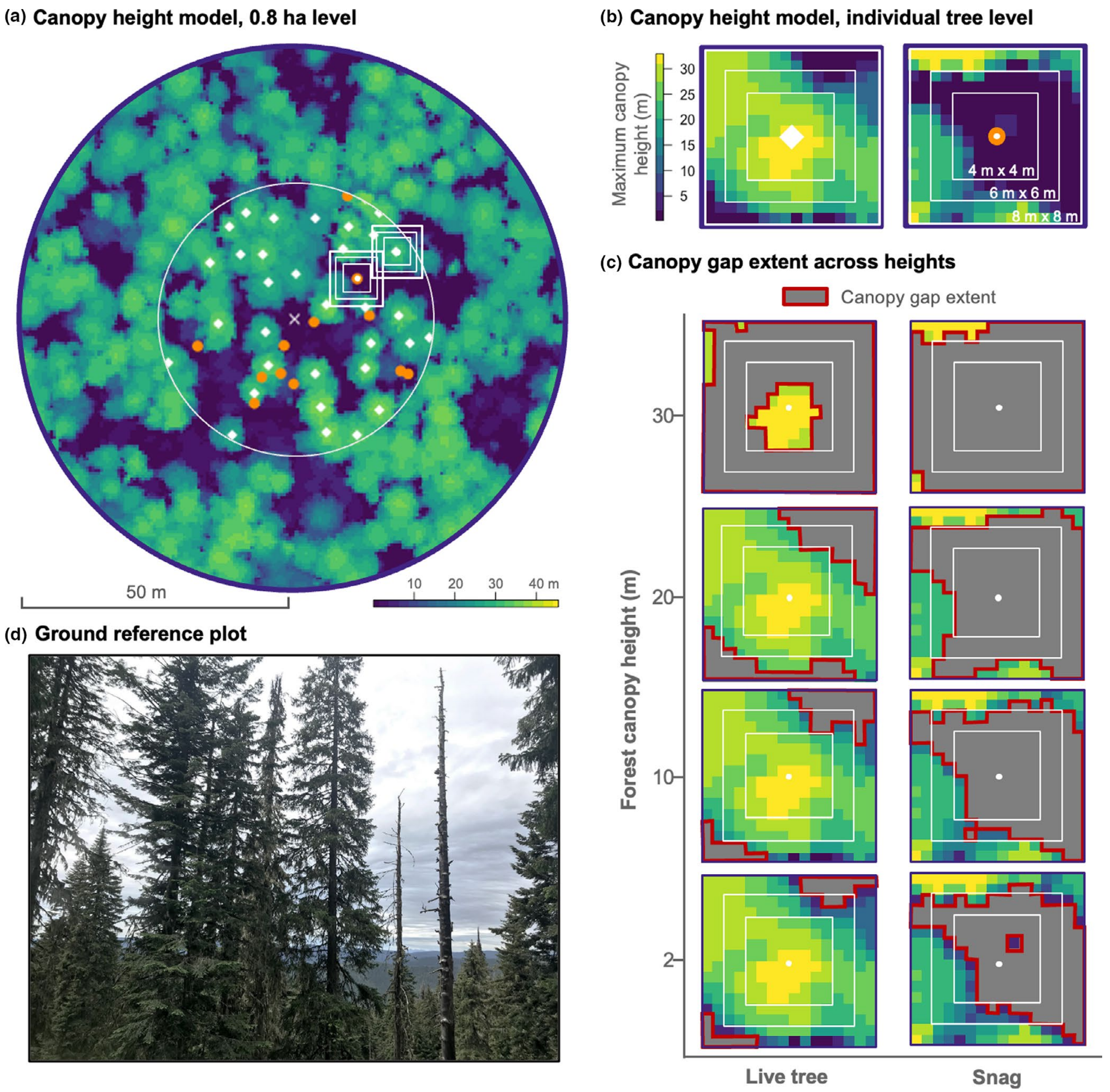

FIGURE 4 Visualization of individual tree-level forest canopy gap detection. Seen from above, (a) airborne lidar-derived canopy height models (CHM; 0.5-m grid cell) were generated at a 50-m radius level and clipped around each individual tree within 25-m radius ground reference plots, based on ITD-generated live tree (white diamond) and reference snag (orange circle) locations. (b) Representative CHMs for a live tree (left) and snag (right) clipped around tree centre (white dot) at three sizes (white squares): small (4 m × 4 m), medium (6 m × 6 m) and large (8 m × 8 m). (c) Forest canopy gaps (grey with red outline) were detected at 25 heights in the forest canopy; here we show four heights: 2 m, 10 m, 20 m and 30 m above-ground for a live tree (left column) and snag (right column). (d) An image taken from a representative ground reference plot, depicting both live trees and snags

distinct patterns that differed ($p < 0.0001$) between snags and live trees for each variable (Figure 5).

The fraction of gaps around both snags and live trees increased with height (Figure 5). At 2-m above-ground, snags showed mean canopy gap fractions ranging from 0.05 to 0.21, compared to live trees with mean canopy gap fractions ranging from 0 to 0.03. Mean canopy gap fraction approached 1 (≥0.98) at 40 m above-ground for all groups. The shape of the line for mean canopy gap fractions across heights (i.e. slope) was similar across tree types. Both snags and live trees followed a sigmoidal curve in gap fraction as height increased (i.e. slope started steep lower in the canopy, flattened in the mid-canopy, then rose steeply again higher in the canopy), though this curve was more pronounced for live trees relative to snags at both sites.

Mean canopy gap fractions showed distinct trends by site as well, with higher canopy gap fractions at the CdA site relative to StJ for both snags (13% higher at CdA) and live trees (2% higher at CdA; Figure 5). Mean canopy gap fractions differed by footprint size for live trees, increasing as footprint size increased (5% increase from small to medium, 4% increase from medium to large; Figure 5). However, this pattern was not seen with snags; mean canopy gap fractions around snags remained consistent across all three footprint sizes (0.1% increase from small to medium, 0.04% decrease from medium to large footprint size).

By focusing on mean differences in canopy gap fractions between snags and live trees at each height (mean snag–mean live tree, from 2 m to 50 m above-ground), further distinctions within the canopy space can be discerned (Figure 6). The greatest differences in canopy gap fraction occurred at heights 10 m–30 m above-ground, whereby snags had ~22% more gap area compared to live trees (Figure 6). Differences between snags and live trees were significant ($p < 0.001$) for small and medium footprint sizes at all heights below 28 m (Figure 6).

4 | DISCUSSION

Exploring how empty space is structured around individual trees opens additional avenues of study when collecting lidar-based forest metrics. Our primary objective was to explore whether gap characteristics around individual trees could be quantified and compared between snags and live trees. We hypothesized that the greatest differences in gap characteristics would occur within the mid-canopy strata, and that there would be an optimal footprint size differentiating snags from live trees. Within our study sites, our hypotheses were supported and we found distinct canopy space profiles between snags and live trees, with the largest distinctions found at heights 10 m–30 m above-ground level, greatest for the smallest footprint size (16 m^2).

The largest unexpected result found in this study occurred among snags between sites; snags at StJ had consistently lower gap fractions than snags at CdA. Many factors may account for this

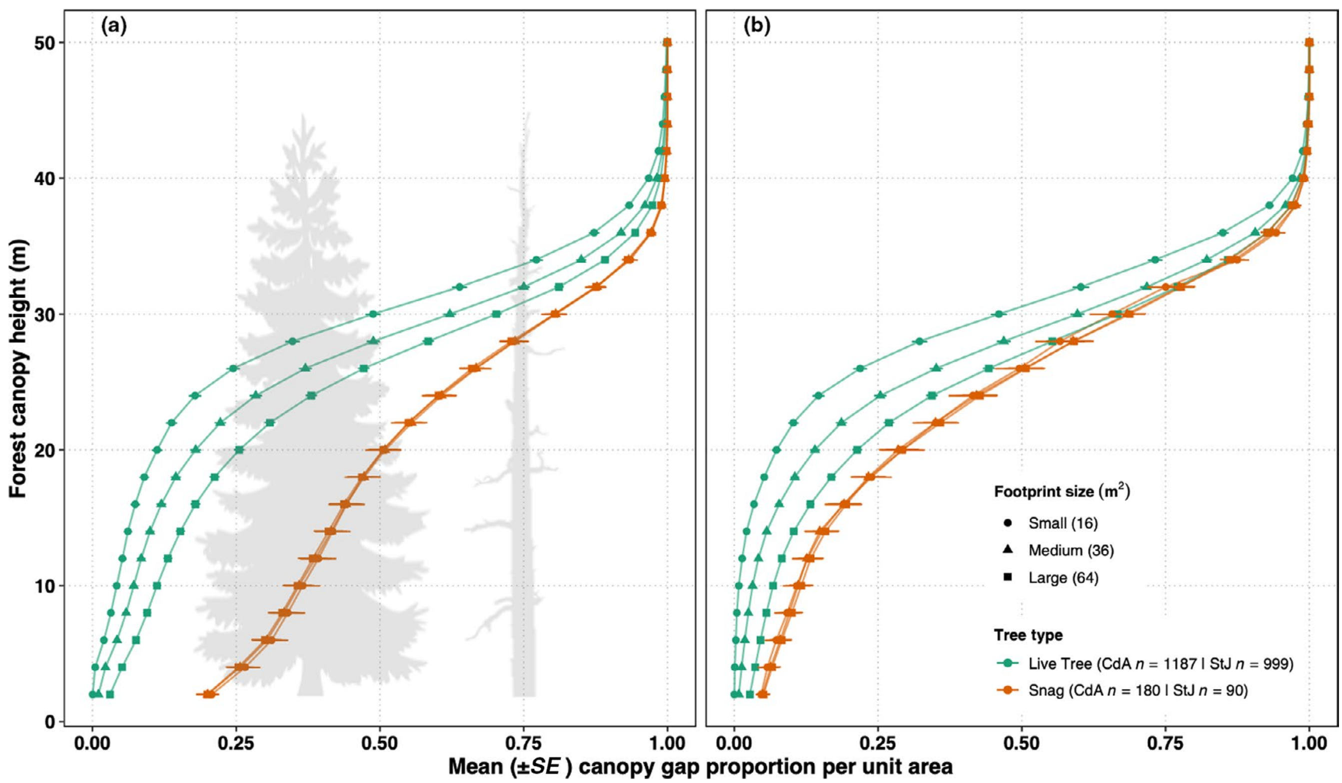

FIGURE 5 Canopy gap fraction around trees by tree type across all forest canopy heights. Mean and standard error are shown for snags (orange) and live trees (green) at each forest canopy height and footprint size, with plots separated by study site: (a) Coeur d'Alene River (CdA) and (b) Saint Joe (StJ) Ranger Districts

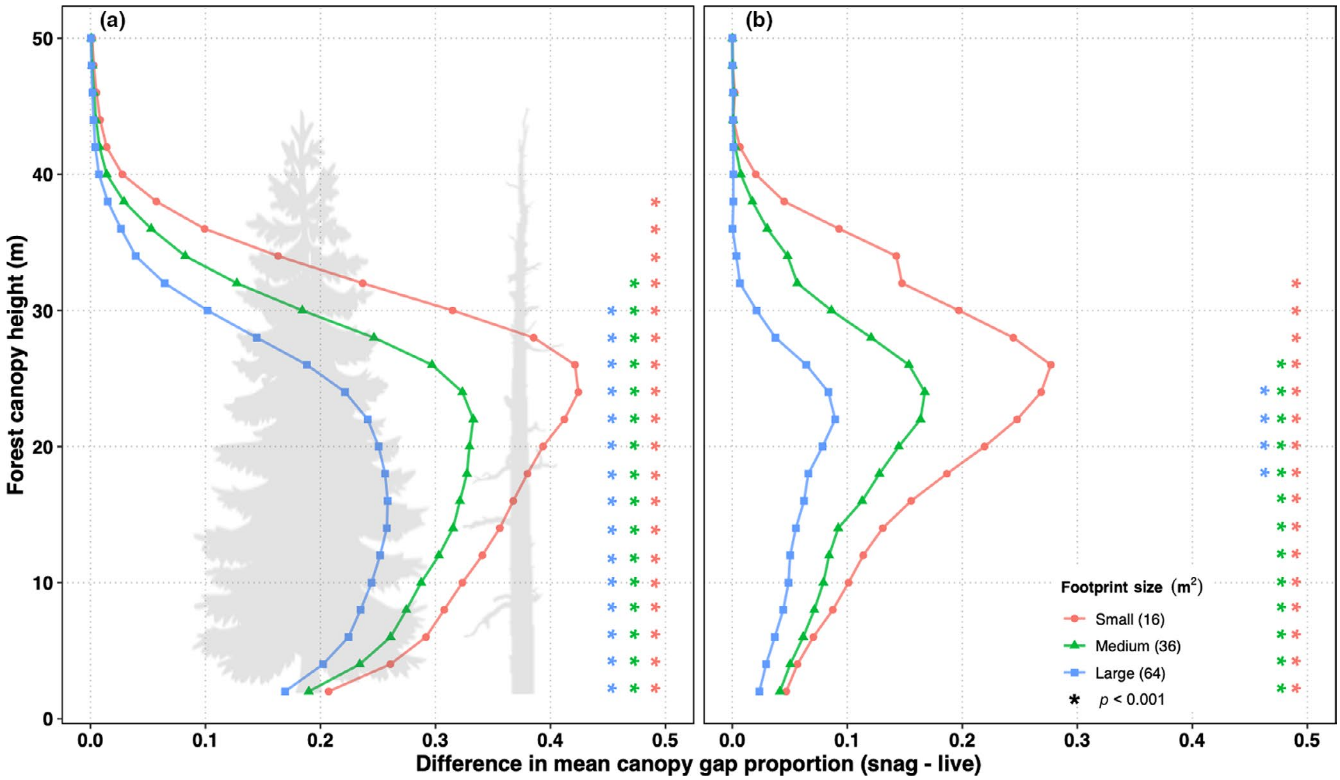

FIGURE 6 Difference in average gap fraction (snag – live) across all forest canopy heights, by site and footprint size. For each height from 2 m to 50 m, the average live tree gap fraction was subtracted from the average snag gap fraction across each footprint size (small [red], medium [green] and large [blue]) at each study site: (a) Coeur d'Alene River (CdA) and (b) Saint Joe (StJ) Ranger Districts. Differences between tree types that were significant ($p < 0.001$) are marked with color-coded asterisks at each height by footprint size, shown on the right of each graph

difference. For instance, differences in gaps around snags across the two sites could simply reflect an effect of tree density, as StJ had greater average stem density in plots than CdA (Table 2) leading to less open area. Stand-level differences in gaps could also be driven by broader sitewide factors such as disturbance history, causes of tree mortality, successional stage and stand age and/or tree species composition (Lefsky et al., 1999). How these stand-level characteristics affect gaps at the individual tree level requires expanded analyses beyond the scope of this study, however.

This study establishes the importance, feasibility and utility of investigating associations between canopy gap structure, live trees and snags at the individual tree level using airborne lidar. The results of this study contribute to the strong foundation of canopy gap research that integrates remote sensing with studies of forest structure and successional processes (e.g. Lefsky et al., 1999). Assessment of the ecological value of canopy gaps has been well studied (Canham, 1988; Spies et al., 1990; Whitmore, 1989), and more recent investigations apply remote sensing tools to monitor biodiversity linked to canopy gaps (Bagaram et al., 2018), study the gap sizes and distribution related to forest stand characteristics and processes (e.g. Asner et al., 2013) and identify and quantify gaps using remote sensing (e.g. Bagaram et al., 2018; Bonnet et al., 2015; Silva et al., 2019; White et al., 2018).

Focusing on canopy gaps around individual trees may not be feasible when dealing with dense forests in an applied context, so the next step will be to evaluate the relationship between canopy gaps and snags at the plot level. This brings in the added challenge of distinguishing gaps around snags from 'true' canopy gaps, where there are no standing trees or snags. We suggest that this can be achieved by focusing on one or two heights above-ground that strongly differentiate snags from live trees and constraining canopy gap area (as true gaps may have larger total areas): for example, evaluating gaps at heights 10 m and 20 m above-ground, constrained to 25%–75% gap fraction of the small footprint size (equal to a gap area of 4 m^2–12 m^2 only). We note that this suggestion is based on one forest type, though this methodology could provide additional benefit from comparisons of canopy gap profiles across multiple forest types. Furthermore, the ForestGapR package (Silva et al., 2019) contains additional functions not applied here, including a function for change detection that could provide greater information and distinction between snags and true gaps by evaluating change in gap extent across selected heights or height percentiles within the canopy. Future studies could employ a standardized method to evaluate gap fractions across multiple forest types: calculating gap fraction at 10 m height in the canopy on a gridded map (2 m × 2 m pixels), then flagging pixels with higher than average gap fraction for the given forest type. If the gap of a given pixel does not extend fully to the ground (a gap fraction of 1.0 at <2 m above-ground, indicating a true gap), it may suggest snag presence.

Fusing previous lidar-based snag modelling approaches with canopy gap analyses such as the ones we have described might provide a promising next step in advancing our understanding of snag distributions in forested landscapes. Prior methods have modelled snags using stand-level lidar-derived metrics focused on structure-based values, via ordinal regression (Bater et al., 2009) or Random Forest classification (Martinuzzi et al., 2009), and intensity-based values via neighbourhood attribute filtering (Wing et al., 2015). Another approach may be to first identify gaps and use them to filter lidar point clouds before beginning more targeted snag modelling, implementing any of the prior methods discussed above. This would serve to pare down the overall file size needed for further processing, improve the speed and/or expand the spatial extent of analyses to potentially improve overall accuracy of snag mapping. Distinctions in canopy space profiles between live trees and snags were robust enough at the single tree level that we suggest incorporating canopy gap evaluation into snag modelling methods in some form.

These methods and the information they provide about the space around trees can help better characterize canopy gaps in dense forests where tree segmentation methods may be less robust due to fewer returns penetrating closed canopy. One of the problems previously reported in mapping snags using airborne lidar was the limited number of returns (e.g. Martinuzzi et al., 2009), likely due to the reduced physical structure of a snag relative to a live tree canopy. Our study found snags to have overall point densities around 25% lower than live trees (Table 4), and several snags had fewer than 100 returns in total. Reframing the problem of fewer returns in the context of canopy gap analysis may help tease apart true gaps from gaps containing snags.

TABLE 4 Average lidar point densities around individual trees across three footprint sizes. After ITD methods were calibrated at the 0.04-ha subplot level, probable live tree locations were generated for each 0.2-ha survey plot, and the central coordinates of those ITD-generated trees were used as the basis for clipping the lidar point clouds around live trees for each footprint size. Field-derived reference snag central coordinates were used as the basis for clipping the lidar point clouds around snags for each footprint size. The number of total returns for each individual tree clip was calculated and divided by the footprint size, for a measure of point density per square metre (mean number of returns ±*SE*). Overall, live trees had higher point densities than snags across all footprint sizes for both sites. Among study sites, point densities were lower around snags at CdA than at StJ

Study site	Footprint size (m^2)	Live tree point density/m^2	Snag point density/m^2
CdA	16	18.5 ± 0.3	10.9 ± 0.5
	36	17.5 ± 0.2	11.1 ± 0.5
	64	16.4 ± 0.2	11.2 ± 0.5
StJ	16	17.1 ± 0.3	14.3 ± 0.7
	36	15.9 ± 0.2	13.9 ± 0.5
	64	14.8 ± 0.2	13.6 ± 0.4

5 | CONCLUSIONS

Canopy gaps and snags are both important elements of forest structure and canopy architecture, and both have ties to successional and disturbance regimes. Use of airborne lidar data can provide a more nuanced understanding of their inter-relatedness and patterns of co-occurrence, which will be of added value to researchers and managers across a range of disciplines. The power of canopy gap analyses coupled with snag detection will only continue to increase as higher resolution airborne lidar surveys are integrated with mobile, terrestrial and UAV-based lidar data collections, and as point cloud analyses become more robust. We urge the consideration of both the presence and absence of data found within lidar point clouds to gain greater insight into spatial and temporal patterns found throughout forest canopies worldwide.

ACKNOWLEDGEMENTS

We thank the USFS RMRS for providing ALS data of the Idaho Panhandle National Forests, as well as assistance in the field from Ben Bright, Patrick Fekety and John Byrne. This work was supported in part by the NSF Idaho EPSCoR Program and the NASA Idaho Space Grant Consortium, and by a NASA Carbon Monitoring Systems (CMS) Program Award (NNH15AZ06I). The authors would like to thank the anonymous reviewers who provided insightful comments that improved this manuscript.

CONFLICTS OF INTEREST

None declared.

AUTHORS' CONTRIBUTIONS

J.M.S., K.T.V., L.A.V. and A.T.H. were involved in conceiving the idea and designing the study; J.M.S. collected field data on snags, and in conjunction with A.T.H. and the USFS RMRS for field data on live trees; J.M.S. analysed the data, with insight and feedback from all other authors; C.A.S. provided input on data processing and the ForestGapR package; J.M.S. and K.T.V. led the writing of the manuscript. All authors contributed critically to the drafts and gave final approval for publication.

PEER REVIEW

The peer review history for this article is available at https://publons.com/publon/10.1111/2041-210X.13752.

DATA AVAILABILITY STATEMENT

The R code and datasets for processing data are available via the Dryad Digital Repository, https://doi.org/10.5061/dryad.tx95x69xx (Stitt et al., 2021). They are also publicly available via the following GitHub page: https://github.com/jessmstitt/snag-gaps.

ORCID

Jessica M. Stitt https://orcid.org/0000-0002-1023-1115
Andrew T. Hudak https://orcid.org/0000-0001-7480-1458
Carlos A. Silva https://orcid.org/0000-0002-7844-3560
Lee A. Vierling https://orcid.org/0000-0001-5344-1983

REFERENCES

Asbeck, T., Basile, M., Stitt, J., Bauhus, J., Storch, I., & Vierling, K. T. (2020). Tree-related microhabitats are similar in mountain forests of Europe and North America and their occurrence may be explained by tree functional groups. *Trees*, *34*(6), 1453–1466. https://doi.org/10.1007/s00468-020-02017-3

Asner, G. P., Kellner, J. R., Kennedy-Bowdoin, T., Knapp, D. E., Anderson, C., & Martin, R. E. (2013). Forest canopy gap distributions in the southern Peruvian Amazon. *PLoS ONE*, *8*(4), e60875. https://doi.org/10.1371/journal.pone.0060875

Bagaram, M. B., Giuliarelli, D., Chirici, G., Giannetti, F., & Barbati, A. (2018). UAV remote sensing for biodiversity monitoring: Are forest canopy gaps good covariates? *Remote Sensing*, *10*(9), 1397. https://doi.org/10.3390/rs10091397

Basile, M., Asbeck, T., Jonker, M., Knuff, A. K., Bauhus, J., Braunisch, V., Mikusiński, M., & Storch, I. (2020). What do tree-related microhabitats tell us about the abundance of forest-dwelling bats, birds, and insects? *Journal of Environmental Management*, *264*. https://doi.org/10.1016/j.jenvman.2020.110401

Bater, C. W., Coops, N. C., Gergel, S. E., LeMay, V., & Collins, D. (2009). Estimation of standing dead tree class distributions in northwest coastal forests using lidar remote sensing. *Canadian Journal of Forest Research*, *39*(6), 1080–1091. https://doi.org/10.1139/X09-030

Bonnet, S., Gaulton, R., Lehaire, F., & Lejeune, P. (2015). Canopy gap mapping from airborne laser scanning: An assessment of the positional and geometrical accuracy. *Remote Sensing*, *7*(9), 11267–11294. https://doi.org/10.3390/rs70911267

Bunnell, F. L., Kremsater, L. L., & Wind, E. (1999). Managing to sustain vertebrate richness in forests of the Pacific Northwest: Relationships within stands. *Environmental Reviews*, *7*(3), 97–146. https://doi.org/10.1139/a99-010

Canham, C. D. (1988). Growth and canopy architecture of shade-tolerant trees: Response to canopy gaps. *Ecology*, *69*(3), 786–795. https://doi.org/10.2307/1941027

Casas, Á., García, M., Siegel, R. B., Koltunov, A., Ramírez, C., & Ustin, S. (2016). Burned forest characterization at single-tree level with airborne laser scanning for assessing wildlife habitat. *Remote Sensing of Environment*, *175*, 231–241. https://doi.org/10.1016/j.rse.2015.12.044

Cockle, K. L., Martin, K., & Wesołowski, T. (2011). Woodpeckers, decay, and the future of cavity-nesting vertebrate communities worldwide. *Frontiers in Ecology and the Environment*, *9*(7), 377–382. https://doi.org/10.1890/110013

Curtis, P. S. (2008). Estimating aboveground carbon in live and standing dead trees. In C. M. Hoover (Ed.), *Field measurements for forest carbon monitoring* (pp. 39–44). Springer.

Drever, M. C., Aitken, K. E., Norris, A. R., & Martin, K. (2008). Woodpeckers as reliable indicators of bird richness, forest health and harvest. *Biological Conservation*, *141*(3), 624–634. https://doi.org/10.1016/j.biocon.2007.12.004

Drever, M. C., & Martin, K. (2010). Response of woodpeckers to changes in forest health and harvest: Implications for conservation of avian biodiversity. *Forest Ecology and Management*, *259*(5), 958–966. https://doi.org/10.1016/j.foreco.2009.11.038

Dudley, J. G., & Saab, V. (2003). *A field protocol to monitor cavity-nesting birds*. United States Department of Agriculture, Forest Service, Rocky Mountain Research Station.

Eitel, J. U. H., Höfle, B., Vierling, L. A., Abellán, A., Asner, G. P., Deems, J. S., Glennie, C. L., Joerg, P. C., LeWinter, A. L., Magney, T. S., Mandlburger, G., Morton, D. C., Müller, J., & Vierling, K. T. (2016). Beyond 3-D: The new spectrum of lidar applications for earth and ecological sciences. *Remote Sensing of Environment*, *186*, 372–392. https://doi.org/10.1016/j.rse.2016.08.018

Falkowski, M. J., Evans, J. S., Martinuzzi, S., Gessler, P. E., & Hudak, A. T. (2009). Characterizing forest succession with lidar data: An evaluation for the Inland Northwest, USA. *Remote Sensing of Environment*, *113*(5), 946–956. https://doi.org/10.1016/j.rse.2009.01.003

Fekety, P. A., Falkowski, M. J., Hudak, A. T., Jain, T. B., & Evans, J. S. (2018). Transferability of lidar-derived basal area and stem density models within a northern Idaho ecoregion. *Canadian Journal of Remote Sensing*, *44*(2), 131–143. https://doi.org/10.1080/07038992.2018.1461557

Gentry, D. J., & Vierling, K. T. (2008). Reuse of woodpecker cavities in the breeding and non-breeding seasons in old burn habitats in the Black Hills, South Dakota. *The American Midland Naturalist*, *160*(2), 413–429. https://doi.org/10.1674/0003-0031(2008)160%5B413:ROWCIT%5D2.0.CO;2

Goetz, S., & Dubayah, R. (2011). Advances in remote sensing technology and implications for measuring and monitoring forest carbon stocks and change. *Carbon Management*, *2*(3), 231–244. https://doi.org/10.4155/cmt.11.18

Guo, X., Coops, N. C., Tompalski, P., Nielsen, S. E., Bater, C. W., & Stadt, J. J. (2017). Regional mapping of vegetation structure for biodiversity monitoring using airborne lidar data. *Ecological Informatics*, *38*, 50–61. https://doi.org/10.1016/j.ecoinf.2017.01.005

Hansen, A. J., Spies, T. A., Swanson, F. J., & Ohmann, J. L. (1991). Conserving biodiversity in managed forests. *BioScience*, *41*(6), 382–392. https://doi.org/10.2307/1311745

Hanula, J. L., Horn, S., & Wade, D. D. (2006). The role of dead wood in maintaining arthropod diversity. In *Insect biodiversity and dead wood: Proceedings of a symposium for the 22nd International Congress of Entomology* (Vol. 93, p. 57). US Department of Agriculture, Forest Service, Southern Research Station.

Idaho Department of Fish and Game (IDFG). (2016). *Idaho species of greatest conservation need*. Idaho Department of Fish and Game. Retrieved from https://idfg.idaho.gov/species/taxa/list/sgcn

Jackson, J. A., & Jackson, B. J. (2004). Ecological relationships between fungi and woodpecker cavity sites. *The Condor*, *106*(1), 37–49. https://doi.org/10.1093/condor/106.1.37

Janssen, P., Hébert, C., & Fortin, D. (2011). Biodiversity conservation in old-growth boreal forest: Black spruce and balsam fir snags harbour distinct assemblages of saproxylic beetles. *Biodiversity and Conservation*, *20*(13), 2917–2932. https://doi.org/10.1007/s10531-011-0127-8

Kankare, V., Holopainen, M., Vastaranta, M., Puttonen, E., Yu, X., Hyyppä, J., Vaaja, M., Hyyppä, H., & Alho, P. (2013). Individual tree biomass estimation using terrestrial laser scanning. *ISPRS Journal of Photogrammetry and Remote Sensing*, *75*, 64–75. https://doi.org/10.1016/j.isprsjprs.2012.10.003

Klockow, P. A., Putman, E. B., Vogel, J. G., Moore, G. W., Edgar, C. B., & Popescu, S. C. (2020). Allometry and structural volume change of standing dead southern pine trees using non-destructive terrestrial LiDAR. *Remote Sensing of Environment*, *241*. https://doi.org/10.1016/j.rse.2020.111729

Krzystek, P., Serebryanyk, A., Schnörr, C., Červenka, J., & Heurich, M. (2020). Large-scale mapping of tree species and dead trees in Šumava National Park and Bavarian Forest National Park using lidar and multispectral imagery. *Remote Sensing*, *12*(4), 661. https://doi.org/10.3390/rs12040661

Larrieu, L., Paillet, Y., Winter, S., Bütler, R., Kraus, D., Krumm, F., Lachat, T., Michel, A. K., Regnery, B., & Vandekerkhove, K. (2018). Tree related microhabitats in temperate and Mediterranean European forests: A hierarchical typology for inventory standardization. *Ecological Indicators*, *84*, 194–207. https://doi.org/10.1016/j.ecolind.2017.08.051

Lefsky, M. A., Cohen, W. B., Acker, S. A., Parker, G. G., Spies, T. A., & Harding, D. (1999). Lidar remote sensing of the canopy structure and biophysical properties of Douglas-fir western hemlock

forests. *Remote Sensing of Environment*, *70*(3), 339–361. https://doi.org/10.1016/S0034-4257(99)00052-8
Lovett, G. M., Arthur, M. A., Weathers, K. C., & Griffin, J. M. (2010). Long-term changes in forest carbon and nitrogen cycling caused by an introduced pest/pathogen complex. *Ecosystems*, *13*(8), 1188–1200. https://doi.org/10.1007/s10021-010-9381-y
Martin, K., Aitken, K. E., & Wiebe, K. L. (2004). Nest sites and nest webs for cavity-nesting communities in interior British Columbia, Canada: Nest characteristics and niche partitioning. *The Condor*, *106*(1), 5–19. https://doi.org/10.1093/condor/106.1.5
Martin, K., & Eadie, J. M. (1999). Nest webs: A community-wide approach to the management and conservation of cavity-nesting forest birds. *Forest Ecology and Management*, *115*(2–3), 243–257. https://doi.org/10.1016/S0378-1127(98)00403-4
Martinuzzi, S., Vierling, L. A., Gould, W. A., Falkowski, M. J., Evans, J. S., Hudak, A. T., & Vierling, K. T. (2009). Mapping snags and understory shrubs for a LiDAR-based assessment of wildlife habitat suitability. *Remote Sensing of Environment*, *113*(12), 2533–2546. https://doi.org/10.1016/j.rse.2009.07.002
Michel, A. K., & Winter, S. (2009). Tree microhabitat structures as indicators of biodiversity in Douglas-fir forests of different stand ages and management histories in the Pacific Northwest, USA. *Forest Ecology and Management*, *257*(6), 1453–1464. https://doi.org/10.1016/j.foreco.2008.11.027
Mikusiński, G., Gromadzki, M., & Chylarecki, P. (2001). Woodpeckers as indicators of forest bird diversity. *Conservation Biology*, *15*(1), 208–217. https://doi.org/10.1111/j.1523-1739.2001.99236.x
Paillet, Y., Archaux, F., Boulanger, V., Debaive, N., Fuhr, M., Gilg, O., Gosselin, F., & Guilbert, E. (2017). Snags and large trees drive higher tree microhabitat densities in strict forest reserves. *Forest Ecology and Management*, *389*, 176–186. https://doi.org/10.1016/j.foreco.2016.12.014
Popescu, S. C., Wynne, R. H., & Nelson, R. F. (2003). Measuring individual tree crown diameter with lidar and assessing its influence on estimating forest volume and biomass. *Canadian Journal of Remote Sensing*, *29*(5), 564–577. https://doi.org/10.5589/m03-027
Powers, E. M., Marshall, J. D., Zhang, J., & Wei, L. (2013). Post-fire management regimes affect carbon sequestration and storage in a Sierra Nevada mixed conifer forest. *Forest Ecology and Management*, *291*, 268–277. https://doi.org/10.1016/j.foreco.2012.07.038
Putman, E. B., Popescu, S. C., Eriksson, M., Zhou, T., Klockow, P., Vogel, J., & Moore, G. W. (2018). Detecting and quantifying standing dead tree structural loss with reconstructed tree models using voxelized terrestrial lidar data. *Remote Sensing of Environment*, *209*, 52–65. https://doi.org/10.1016/j.rse.2018.02.028
R Core Team. (2020). *R: A language and environment for statistical computing*. R Foundation for Statistical Computing. Retrieved from https://www.R-project.org/
Ritchie, M. W., Knapp, E. E., & Skinner, C. N. (2013). Snag longevity and surface fuel accumulation following post-fire logging in a ponderosa pine dominated forest. *Forest Ecology and Management*, *287*, 113–122. https://doi.org/10.1016/j.foreco.2012.09.001
Roussel, J.-R., Auty, D., Coops, N. C., Tompalski, P., Goodbody, T. R. H., Meador, A. S., Bourdon, J.-F., de Boissieu, F., & Achim, A. (2020). lidR: An R package for analysis of Airborne Laser Scanning (ALS) data. *Remote Sensing of Environment*, *251*. https://doi.org/10.1016/j.rse.2020.112061
Russell, M. B., Fraver, S., Aakala, T., Gove, J. H., Woodall, C. W., D'Amato, A. W., & Ducey, M. J. (2015). Quantifying carbon stores and decomposition in dead wood: A review. *Forest Ecology and Management*, *350*, 107–128. https://doi.org/10.1016/j.foreco.2015.04.033
Schroeder, R. L. (1983). *Habitat suitability index models: Downy woodpecker* (Vol. 82). Western Energy and Land Use Team, Division of Biological Services, Research and Development, Fish and Wildlife Service, US Department of the Interior.
Shugart, H. H. (1984). *A theory of forest dynamics. The ecological implications of forest succession models*. Springer-Verlag.
Silva, C. A., Hudak, A. T., Vierling, L. A., Loudermilk, E. L., O'Brien, J. J., Hiers, J. K., … Khosravipour, A. (2016). Imputation of individual longleaf pine (*Pinus palustris Mill.*) tree attributes from field and LiDAR data. *Canadian Journal of Remote Sensing*, *42*(5), 554–573. https://doi.org/10.1080/07038992.2016.1196582
Silva, C. A., Valbuena, R., Pinagé, E. R., Mohan, M., de Almeida, D. R., North Broadbent, E., … Klauberg, C. (2019). ForestGapR: An R Package for forest gap analysis from canopy height models. *Methods in Ecology and Evolution*, *10*(8), 1347–1356. https://doi.org/10.1111/2041-210X.13211
Spies, T. A., Franklin, J. F., & Klopsch, M. (1990). Canopy gaps in Douglas-fir forests of the Cascade Mountains. *Canadian Journal of Forest Research*, *20*(5), 649–658. https://doi.org/10.1139/x90-087
Stitt, J. M., Silva, C. A., Hudak, A. T., Vierling, L. A., & Vierling, K. T. (2021). Data from: Characterizing individual tree-level snags using airborne lidar-derived forest canopy gaps within closed-canopy conifer forests. *Dryad Digital Repository*, https://doi.org/10.5061/dryad.tx95x69xx
Tews, J., Brose, U., Grimm, V., Tielbörger, K., Wichmann, M. C., Schwager, M., & Jeltsch, F. (2004). Animal species diversity driven by habitat heterogeneity/diversity: The importance of keystone structures. *Journal of Biogeography*, *31*(1), 79–92. https://doi.org/10.1046/j.0305-0270.2003.00994.x
Titus, R. (1983). Management of snags and den trees in Missouri – A process. J. W. Davis, G. A. Goodwin, & F. A. Ockenfels (tech. coords.). Gen. Tech. Rep. RM–99, Ft. Collins, CO: US Department of Agriculture. Forest Service, Rocky Mountain Forest and Range Experiment Station, 51–59.
Urban, D. L., O'Neill, R. V., & Shugart Jr., H. H. (1987). A hierarchical perspective can help scientists understand spatial patterns. *BioScience*, *37*(2), 119–127.
Vierling, K. T., Vierling, L. A., Gould, W. A., Martinuzzi, S., & Clawges, R. M. (2008). Lidar: Shedding new light on habitat characterization and modeling. *Frontiers in Ecology and the Environment*, *6*(2), 90–98. https://doi.org/10.1890/070001
Vogeler, J. C., & Cohen, W. B. (2016). A review of the role of active remote sensing and data fusion for characterizing forest in wildlife habitat models. *Revista de Teledetección*, *45*, 1–14. https://doi.org/10.4995/raet.2016.3981
Vogeler, J. C., Hudak, A. T., Vierling, L. A., & Vierling, K. T. (2013). Lidar-derived canopy architecture predicts brown creeper occupancy of two western coniferous forests. *The Condor*, *115*(3), 614–622. https://doi.org/10.1525/cond.2013.110082
White, J. C., Tompalski, P., Coops, N. C., & Wulder, M. A. (2018). Comparison of airborne laser scanning and digital stereo imagery for characterizing forest canopy gaps in coastal temperate rainforests. *Remote Sensing of Environment*, *208*, 1–14. https://doi.org/10.1016/j.rse.2018.02.002
Whitmore, T. (1989). Canopy gaps and the two major groups of forest trees. *Ecology*, *70*(3), 536–538. https://doi.org/10.2307/1940195
Wing, B. M., Ritchie, M. W., Boston, K., Cohen, W. B., & Olsen, M. J. (2015). Individual snag detection using neighborhood attribute filtered airborne lidar data. *Remote Sensing of Environment*, *163*, 165–179. https://doi.org/10.1016/j.rse.2015.03.013
Yao, W., Krzystek, P., & Heurich, M. (2012). Identifying standing dead trees in forest areas based on 3D single tree detection from full waveform lidar data. *ISPRS Annals of the Photogrammetry, Remote Sensing and Spatial Information Sciences*, *1*(7). https://doi.org/10.5194/isprsannals-I-7-359-2012

How to cite this article: Stitt, J. M., Hudak, A. T., Silva, C. A., Vierling, L. A., & Vierling, K. T. (2022). Characterizing individual tree-level snags using airborne lidar-derived forest canopy gaps within closed-canopy conifer forests. *Methods in Ecology and Evolution*, 13, 473–484. https://doi.org/10.1111/2041-210X.13752